Available online at www.sciencedirect.com
ScienceDirect
Journal of Power Sources 162 (2006) 74–80
JOURNAL OF POWER SOURCES
www.elsevier.com/locate/jpowsour

Regenerative, coal-based solid oxide fuel cell-electrolyzers

Srikanth Gopalan *, Guosheng Ye, Uday B. Pal

Department of Manufacturing Engineering, Boston University, 15 Saint Mary's Street, Brookline, MA 02446, USA

Received 11 May 2006; received in revised form 30 June 2006; accepted 3 July 2006
Available online 17 August 2006

Abstract

In this paper we theoretically analyze the concept of a reversible-and-regenerative solid oxide device comprising a multilayer architecture that will employ an oxygen-ion-conducting solid oxide, e.g. yttria-stabilized zirconia (YSZ) as the electrolyte. The two electrodes to be used in the device are reversible, i.e. capable of reversibly operating as the cathode and as the anode. One of the electrodes to be used is a liquid metal Ag and the other electrode will be chosen from several options including a nickel (Ni)–YSZ porous cermet. The advantage of such a device is the ability to use coal (carbon), an abundantly available fuel in a solid oxide fuel cell. The device can be operated in an electrolysis mode to generate hydrogen from coal and steam and in a power generation mode as a solid oxide fuel cell to generate electricity from the hydrogen generated during the electrolysis cycles.

Keywords: Reversible; Fuel cell; Electrolysis; Coal; Ceramic; Liquid metal electrode

1. Introduction

The 2005 hurricanes in the gulf-coast region of the United States resulted in significant loss of refining capacity of the oil industry. These natural disasters have clearly underscored the need to rely on a diversity of energy resources rather than a single resource like oil. The United States has abundant reserves of coal. However, coal is considered to be very polluting because of the amount of SO_x, NO_x, and particulate emissions associated with its combustion.

In this paper we propose a novel approach to utilize coal that would eliminate the combustion process and replace it with a direct electrochemical process to generate hydrogen that can be subsequently used as a fuel to generate electricity by the same device. In the proposed process, when the reversible device is operated as an electrolyzer, steam is fed to the cathode (e.g. Ni–YSZ) side and coal to the anode side of the electrolyzer in the temperature range 900–1000 °C. The following half-cell reactions occur at the cathode and anode of the electrolyzer:

At the cathode:

$$H_2O(g) + 2e^-(Ni) = H_2(g) + O^{2-}(YSZ) \quad (1)$$

At the anode:

$$O^{2-} = [O]_{Ag} + 2e^- \quad (2)$$

Water vapor is electrolyzed at the cathode–electrolyte interface to form hydrogen in the gas phase and oxygen ions, which transport through the electrolyte to the anode. At the anode (which is liquid Ag metal)–electrolyte interface, the oxygen ions liberate two electrons resulting in dissolved oxygen in the liquid Ag metal. The dissolved oxygen migrates through the liquid Ag metal to react with coal (carbon) to form a mixture of CO and CO_2 at the liquid Ag/carbon interface, i.e.

At the liquid Ag/carbon interface:

$$[O]_{Ag} + C = CO(g) \quad (3a)$$

$$2[O]_{Ag} + C = CO_2(g) \quad (3b)$$

The hydrogen on the cathode side can be collected, stored and later used as fuel to operate the same device run in reverse as a fuel cell as shown in Fig. 1.

The electrodes that we propose to use are liquid silver (anode in electrolyzer mode and cathode in fuel cell mode) and nickel–yttria-stabilized zirconia (Ni–YSZ; cathode in electrolyzer mode and anode in fuel cell mode) cermet. Both electrodes are known to be compatible (stable) in contact with the YSZ electrolyte. However, if Ag is utilized as the cathode the

* Corresponding author. Tel.: +1 617 358 2297; fax: +1 617 353 5548.
E-mail address: sgopalan@bu.edu (S. Gopalan).

0378-7753/$ – see front matter © 2006 Published by Elsevier B.V.
doi:10.1016/j.jpowsour.2006.07.001

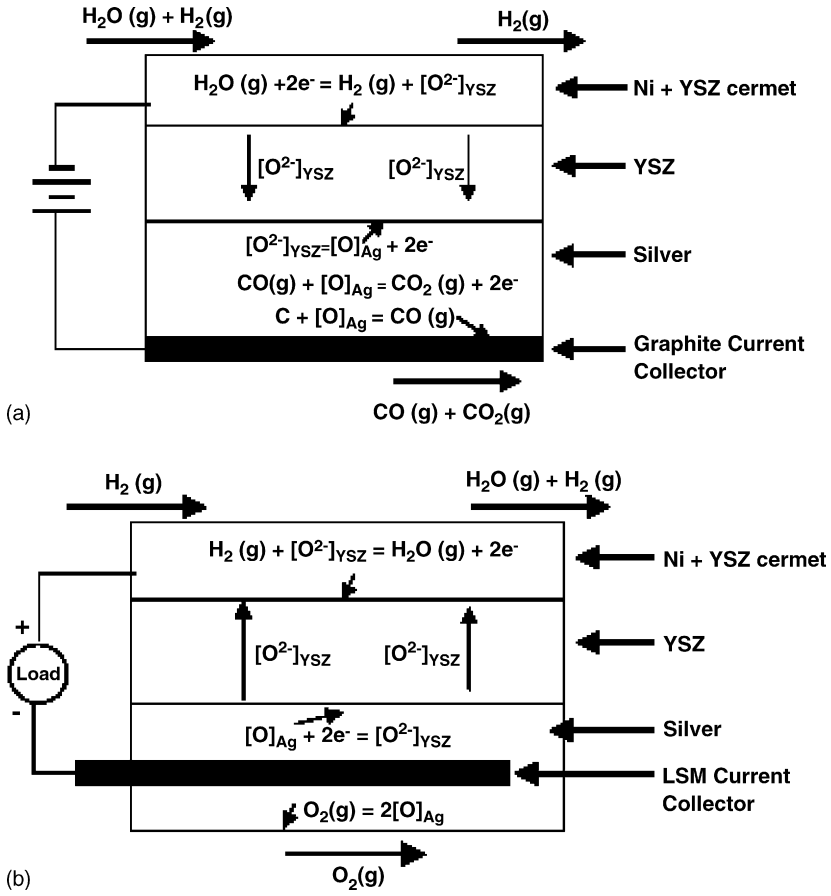

Fig. 1. Concept of the carbon (coal)-based-reversible-and-regenerative SOFC. (a) Carbon (coal)-based electrolyzer for hydrogen production and (b) fuel cell running on hydrogen and oxygen.

operating temperature of the device is expected to be limited to the range of 1235–1300 K, preferably, ∼1273 K. Silver at this temperature will be in the molten state. Although it is an expensive material, the reason for employing liquid silver as one of the electrodes is that it has negligible solubility for carbon [1], high solubility and diffusivity for oxygen [2,3,19], and does not oxidize at these temperatures [4]. Further, a liquid metal electrode provides a very unique feature, namely, a reaction interface for the dissolved oxygen to react with carbon. These unique properties will allow silver to function as an anode in the electrolyzer and as a cathode in the fuel cell (Fig. 1a and b). It is anticipated that enabling the use of coal, an abundant and inexpensive fuel and the high power densities will justify the expense associated with using liquid Ag electrodes, including refining the Ag to remove coal impurities for reuse. The other issue of concern is the ash content of the coal. At higher temperatures, in the absence of oxygen, it produces aromatic hydrocarbons and molten material which decomposes further in an endothermic reaction to produce ash. While this effect has been found in molten carbonate fuel cell (on the anodic side), the effect of the presence of ash in the coal remains to be seen in the case of the present device.

While operating the device as an electrolyzer (Fig. 1a), steam-rich feed (97% steam and 3% H_2) will be circulated over the Ni–YSZ cermet electrode functioning as the cathode; 3% H_2 in the gas mix is necessary to prevent Ni oxidation. Ni or Ni-alloys can be used as the current collectors for the cermet electrode. The steam will be reduced at the cathode producing hydrogen and oxygen ions. The oxygen ions will migrate through the solid YSZ electrolyte towards the liquid silver anode. At the YSZ/silver interface, the oxygen ions will oxidize (lose electrons) and dissolve in silver as neutral oxygen atoms ([O]). Carbon (treated coal) rods will be used as a consumable feed in the silver to oxidize the dissolved oxygen in silver. Carbon rods will also function as current collectors for the liquid silver electrode. The applied electrical potential will depend on the resistive and polarization losses in the electrolyzer, the desired rate of hydrogen production and the corresponding rate of carbon feed. It is to be noted that the applied electrical potential can be increased as long as the concentration polarization at the electrodes does not reduce the oxygen chemical potential on the electrolyte surface to an extent that induces electronic conductivity in the YSZ electrolyte. Based on the information available on the electrochemical performance of Ni–YSZ cermet electrodes and carbon consuming liquid anodes (copper, tin and silver) in contact with YSZ electrolytes [5–11,21], it is expected that ionic current densities on the order of 1 A cm^{-2} can be easily achieved in a well-designed electrolyzer cell. These current densities were obtained on thick-film YSZ electrolytes with thickness of the order of 1 mm. When the electrolyte is made thinner, of the order of a few tens of μm, much higher current densities are expected. Since the silver is thermodynamically stable against oxidation at these temperatures, it is also possible

to operate the electrolyzer without the carbon feed. However, by having the carbon feed in the silver, the off-peak electrical energy needed to produce hydrogen from the steam feed will be greatly reduced. The quantitative details of this effect are presented in Section 2.1.

In the reversible mode, while operating the device as a fuel cell (Fig. 1b), air will be bubbled into the silver through a refractory (alumina) tube. Oxygen will dissolve in the molten silver ([O]) and participate in the cathodic reaction at the YSZ/molten silver interface to generate the oxygen ions. Hydrogen-rich feed will be circulated over the Ni–YSZ cermet electrode (anode) to oxidize the oxygen ions migrating through the YSZ electrolyte. Sintered rods of strontium-doped lanthanum manganite ($La_{1-x}Sr_xMnO_3$) or strontium and cobalt-doped lanthanum ferrite ($La_{1-x}Sr_xCo_yFe_{1-y}O_3$) will dip into the molten silver (functioning as the cathode) to serve as current collectors. LSM and LSCF have both been demonstrated to be excellent cathode materials (electronic conductors under an oxidizing atmosphere) in SOFCs [12–16,20] and laboratory tests indicate that they are stable in contact with silver. Ni or its alloys will serve as the current collector for the Ni–YSZ cermet electrode.

During off-peak periods, the electrochemical cell can be employed for producing hydrogen from carbon (coal) and steam through electrolysis. The hydrogen produced is separated from the carbon (coal) side by the YSZ membrane and can be easily collected in the pure form by condensing out the excess steam. During peak periods the same device can be used as a fuel cell to generate electricity from hydrogen. The device can thus work continuously, alternating between these two modes as required and will not need to be shut down or thermally cycled.

The prospect of eliminating conventional coal gasifiers is particularly attractive for economic and environmental reasons. The CO(g) generated while operating the device as an electrolyzer can be combusted with oxygen to recover the heat for steam generation. The combustion product CO_2(g) can be permanently sequestered in geologic formations. Candidate reservoir(s) could include depleted oil and gas reservoirs, unmineable coal seams, deep saline aquifers, and basalt formations-all common in the United States [17,18]. If needed, some of the CO(g) and excess steam from the electrolyzer can be passed through a water-gas shift reactor to make additional hydrogen ($CO(g) + H_2O(g) \rightarrow CO_2(g) + H_2(g)$). However, in this case the hydrogen produced has to be separated from the CO_2(g) involving additional cost (see Section 2.2).

2. System design and efficiency

2.1. Analysis of electrolyzer efficiency

The suggested process scheme is similar to the one proposed for a methane-assisted steam electrolyzer [22]. However, since coal is used as a starting fuel, the expected efficiency based on lower heating values and energy inputs are somewhat lower compared to methane. In the proposed coal (carbon) electrolyzer, the following half-cell reactions are expected to occur.

At the cathode:

$$H_2O(g) + 2e^-(Ni) \rightarrow H_2(g) + O^{2-}(YSZ) \quad (4)$$

At the anode:

$$O^{2-}(YSZ) \rightarrow O(Ag) + 2e^-(Ag) \quad (5)$$

The oxygen that dissolves in the Ag at the Ag/YSZ is expected to transport through the molten Ag to react with the coal (carbon) to form carbon monoxide or carbon dioxide gas through the following reactions:

$$C(s) + O(Ag) = CO(g) \quad (6)$$

$$C(s) + 2O(Ag) = CO_2(g) \quad (7)$$

At an electrolysis temperature of 1000 °C (1273 K), thermodynamic calculations show that CO(g) is the preferred reaction product on the carbon side of the electrolyzer reaction. The CO generated on the anodic side of the electrolyzer is combusted in a separate catalytic combustion reactor with excess air. The combustion products and the hydrogen rich H_2–H_2O mixture exiting the electrolyzer are heat exchanged with the material inputs to the process, namely coal (carbon) and water. The overall process scheme with heat recovery from post combustion with air is shown in Fig. 2. (Overall process reaction is: $C + H_2O(l) + 1/2O_2(g) \rightarrow CO_2(g) + H_2(g)$; $\Delta H^\circ_{Reaction} = -107$ kJ at 298 K.)

The hydrogen generation energy efficiency is defined by the equation:

$$\eta_{H_2} = \frac{\dot{n}_{H_2}(LHV_{H_2})}{\dot{n}_C(HV_C) + \dot{E}_{el}} \quad (5)$$

In the above equation, η_{H_2} is the hydrogen generation energy efficiency, $\dot{n}_i$s refer to the flux or feed or production rate of species i per unit area of the cell, $\dot{E}_{el}$ is the rate of electrical energy input, LHV_i and HV_i are the lower heating value and heating value of the species 'i', respectively. Eq. (5) is nearly identical to the efficiency definition given by Martinez-Frias et al. for their methane-assisted steam electrolysis process [22]. The rate of electrical energy input to the electrolyzer, $\dot{E}_{el}$ is given by:

$$\dot{E}_{el} = E_{app} i \quad (6)$$

If the electrode polarization losses are incorporated, the current density can be expressed as:

$$i = \frac{E_{app} + E_{Nernst}}{R_i + R_p} \quad (7)$$

where E_{app} (volts) is the externally applied voltage, E_{Nernst} (volts) the Nernst potential across the YSZ membrane for the reaction $C + H_2O(g) = CO(g) + H_2(g)$ and R_i ($\Omega\,cm^2$) is the area specific resistance of the electrolyzer cell. To calculate the hydrogen generation energy efficiency we need to formulate heat and mass balances across the system, the catalytic reactor, and the heat exchanger (in terms of its effectiveness). This is presented in the following.

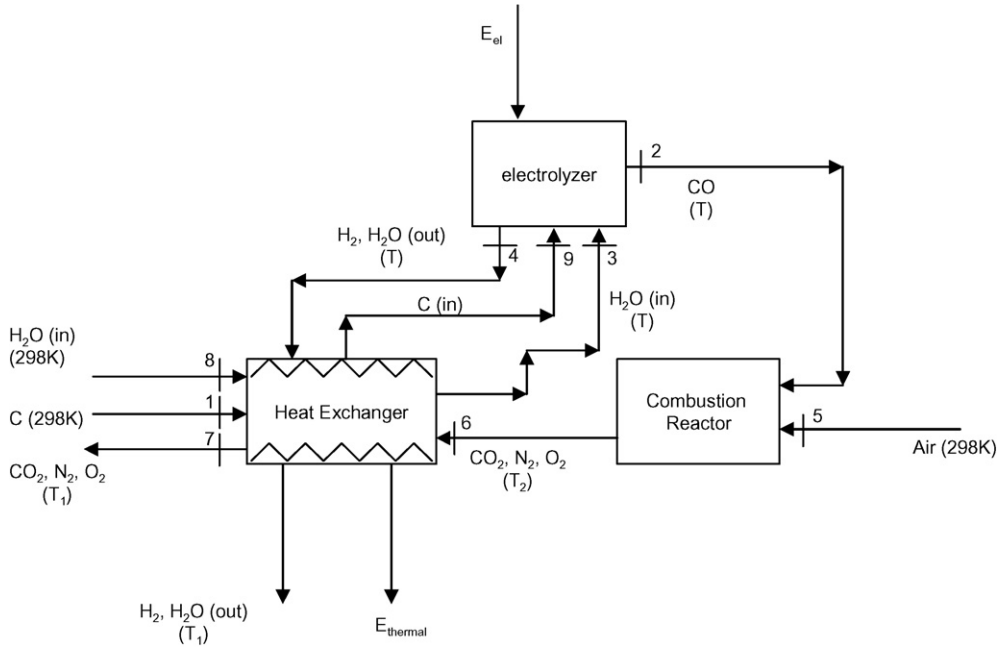

Fig. 2. Process scheme involving the electrolyzer operating on coal and steam.

The heat balance across the entire system can be written as:

$$\dot{n}_{\mathrm{C}} H_{\mathrm{C}}^{298\mathrm{K}} + \dot{n}_{\mathrm{H_2O(in)}} H_{\mathrm{H_2O}}^{298\mathrm{K}} + \dot{n}_{\mathrm{air}} H_{\mathrm{air}}^{298\mathrm{K}} + \dot{E}_{\mathrm{el}} = \dot{n}_{\mathrm{CO_2}} H_{\mathrm{CO_2}}^{T_1} + \dot{n}_{\mathrm{N_2}} H_{\mathrm{N_2}}^{T_1} + \dot{n}_{\mathrm{O_2}} H_{\mathrm{O_2}}^{T_1} + \dot{n}_{\mathrm{H_2}} H_{\mathrm{H_2}}^{T_1} + \dot{n}_{\mathrm{H_2O(out)}} H_{\mathrm{H_2O}}^{T_1} + \dot{E}_{\mathrm{thermal}} \quad (8)$$

The heat exchanger effectiveness is given by:

$$\varepsilon = \frac{\dot{n}_{\mathrm{H_2O(in)}}(H_{\mathrm{H_2O}}^{T} - H_{\mathrm{H_2O}}^{298\mathrm{K}}) + \dot{E}_{\mathrm{thermal}} + \dot{n}_{\mathrm{C}}(H_{\mathrm{C}}^{T} - H_{\mathrm{C}}^{298})}{(\dot{n}_{\mathrm{CO_2}} H_{\mathrm{CO_2}}^{T_2} + \dot{n}_{\mathrm{N_2}} H_{\mathrm{N_2}}^{T_2} + \dot{n}_{\mathrm{O_2}} H_{\mathrm{O_2}}^{T_2}) - (\dot{n}_{\mathrm{CO_2}} H_{\mathrm{CO_2}}^{T_1} + \dot{n}_{\mathrm{N_2}} H_{\mathrm{N_2}}^{T_1} + \dot{n}_{\mathrm{O_2}} H_{\mathrm{O_2}}^{T_1}) + \dot{n}_{\mathrm{H_2O(out)}}(H_{\mathrm{H_2O}}^{T} - H_{\mathrm{H_2O}}^{T_1}) + \dot{n}_{\mathrm{H_2}}(H_{\mathrm{H_2}}^{T} - H_{\mathrm{H_2}}^{T_1})} \quad (9)$$

In Eqs. (8) and (9), $\dot{E}_{\mathrm{thermal}}$ is the total heat rejection from the heat exchanger which is available for other uses; $H_i^{T_j}$ is the enthalpy of species 'i' at the temperature T_j. For these calculations, it is assumed that the heat exchanger effectiveness is 85% ($\varepsilon = 0.85$), the heat exchanger exit temperature (T_1) is 500 K and the electrolyzer is operated at a temperature (T) of 1300 K. The actual process is expected to use excess steam to minimize concentration polarization. The process flows for the calculation are adjusted such that the inlet flow on the cathodic side of the electrolyzer comprises 97% H_2O–3% H_2 and the exit flow depleted in steam comprises 97% H_2–3% H_2O. The oxygen partial pressure on the cathodic side of the electrolyzer is fixed by the H_2–H_2O equilibrium and that on the anodic side by the C–CO equilibrium. Assuming that CO bubbles precipitate within the liquid Ag metal at 1 atm and assuming that solid carbon dipped in the liquid Ag metal is always present during the electrolysis process, the inlet Nernst potential at the operating temperature of 1300 K is 0.458 V and the exit Nernst potential is 0.066 V leading to an average Nernst potential of 0.262 V [23]. Thus an average E_{Nernst} at 1300 K of 0.262 V was used in the present calculations.

An energy balance across the catalytic reactor assuming adiabatic conditions gives:

$$\dot{n}_{\mathrm{air}} H_{\mathrm{air}}^{298\mathrm{K}} + \dot{n}_{\mathrm{CO}} H_{\mathrm{CO}}^{T} = \dot{n}_{\mathrm{CO_2}} H_{\mathrm{CO_2}}^{T_2} + \dot{n}_{\mathrm{O_2}} H_{\mathrm{O_2}}^{T_2} + \dot{n}_{\mathrm{N_2}} H_{\mathrm{N_2}}^{T_2} \quad (10)$$

In Eq. (10), the last two terms on the right hand side arise from excess (over-stoichiometric) air; for the purpose of calculations 10% excess air is used for the combustion reaction. Further, relating the carbon consumption rate per unit electrolyzer electrode area $\dot{n}_{\mathrm{C}}$, and the hydrogen flux $\dot{n}_{\mathrm{H_2}}$ to the current density i through the electrolyzer, it is possible to write:

$$\dot{n}_{\mathrm{C}} = \dot{n}_{\mathrm{H_2}} = \frac{i}{2F} \quad (11)$$

where F is the Faraday constant (96,487 C). The inputs air, H_2O(l) and carbon are all assumed to enter the process at 298 K, and the area specific resistance of the cell at the operating temperature of the electrolyzer (1300 K) is assumed to be 0.3 Ω cm^2. The calculated hydrogen generation energy efficiency from Eq. (5) plotted as a function of current density 'i', for different assumed values of the polarization resistance of the cell R_{p}, is shown in Fig. 3a. It is evident that the total resistance of the cell $R_i + R_{\mathrm{p}}$ has a dramatic effect on the hydrogen generation efficiency. A higher total cell resistance leads to increased polarization losses in the cell and a net decrease in the hydrogen generation efficiency. The definition of the energy efficiency Eq. (5) does not consider the efficiency of electrical power generation at the source of the electrical power used in the electrolysis

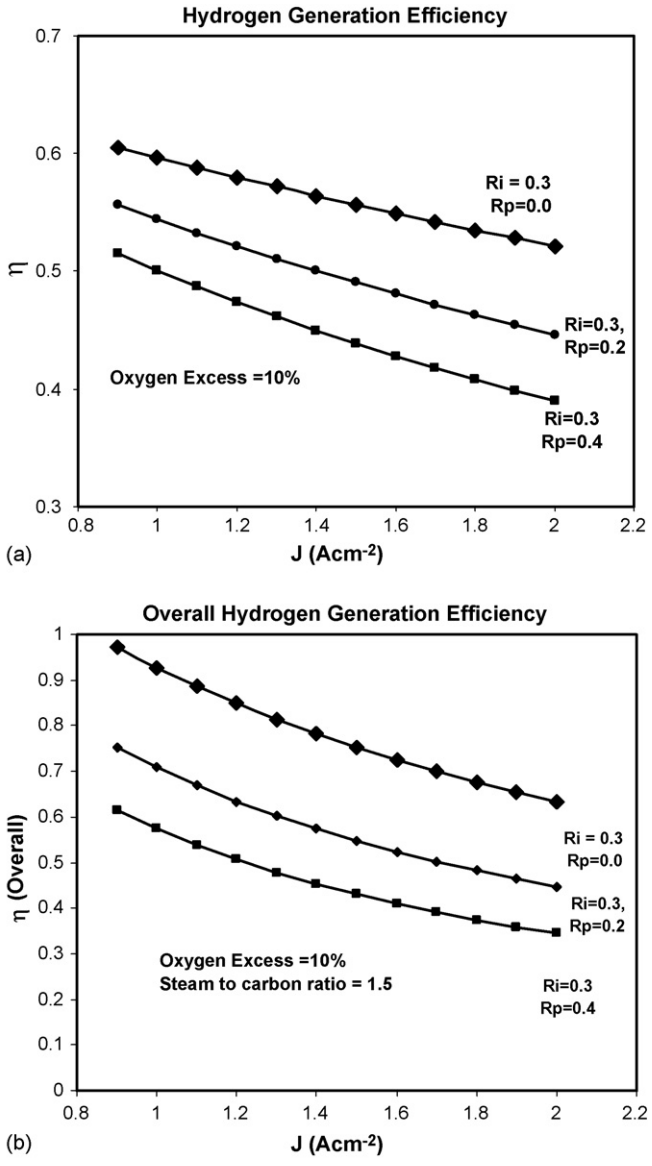

Fig. 3. (a) Hydrogen generation energy efficiency (Eq. (5)) as a function of current density and (b) overall energy efficiency as a function of current density (Eq. (12)). Calculation assumptions: electrolyzer at 1300 K; exit flow 373 K; inlet flow 298 K; 10% oxygen excess for combustion.

process and the extra thermal energy from the heat exchanger, namely $\dot{E}_{\text{thermal}}$ that is available for other uses such as space heating. To obtain the overall energy efficiency of the proposed process scheme, taking into account the efficiency of power generation and the extra thermal energy, one could define an alternate measure of efficiency, namely,

$$\eta_{\text{overall}} = \frac{\dot{n}_{H_2}(\text{LHV}_{H_2}) + \dot{E}_{\text{thermal}}}{\dot{n}_C(\text{HV}_C) + \dot{E}_{\text{el}}/\eta_{\text{elc}}} \tag{12}$$

This assumes that $\dot{E}_{\text{thermal}}$ from the heat exchanger is available for use. Thus, the overall energy efficiency of the proposed scheme shown in Fig. 3b as a function of various polarization resistances is higher than the hydrogen energy generation efficiency shown in Fig. 3a. On an industrial scale this is considered to be quite attractive since the maximum theoretical

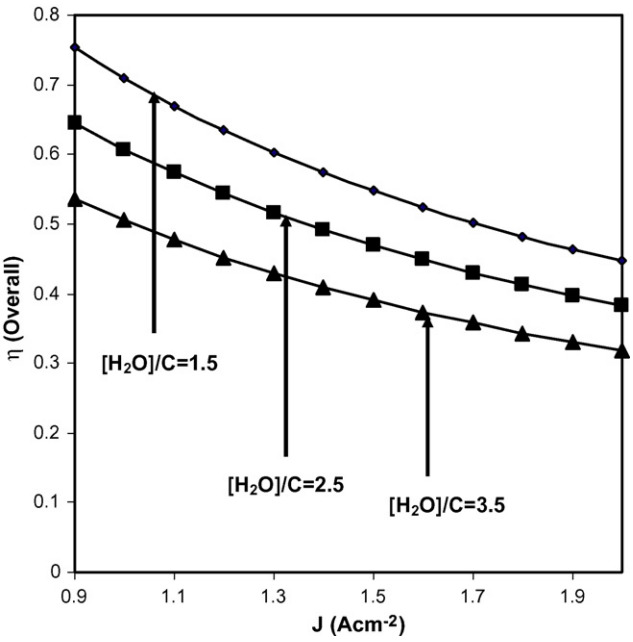

Fig. 4. Overall efficiency versus current density for various steam-to-carbon ratios.

hydrogen generation energy efficiency possible with C and steam is $2\text{LHV}_{H_2}/\text{HV}_C + \Delta H_{\text{reaction}} = 0.837$ or 83.7% based on the reaction $C + 2H_2O(l) \rightarrow CO_2(g) + 2H_2(g)$. Fig. 4 shows a plot of η_{overall} as a function of current density at fixed ohmic and polarization resistances for various values of the steam-to-carbon ratio. As seen, η_{overall} decreases with increasing steam-to-carbon ratio. An inspection of Eq. (12) reveals the reason. The carbon feed rate per unit cell area is fixed by the operating current density of the cell through Eq. (11). Thus increasing the steam-to-carbon ratio at a fixed current density is tantamount to increasing the steam flow at a fixed carbon feed rate. The increasing steam input into the electrolyzer necessitates that a greater portion of the thermal energy from the exhaust of the catalytic combustor, and that from the steam–hydrogen mixture (enriched in hydrogen) exiting the electrolyzer, be used to evaporate and heat the water input into the system at 298 K. Thus the net extra thermal energy E_{thermal} from the heat exchanger available for other uses like space heating decreases with increasing steam flow as seen in Fig. 5.

The proposed process can be altered to include a water-gas shift reactor ($CO(g) + H_2O(g) \rightarrow CO_2(g) + H_2(g)$) to generate additional hydrogen from some of the CO(g) and the excess steam that exits the electrolyzer. However, this would involve an additional step of separating hydrogen from $CO_2(g)$ and may not be justified from the standpoint of the overall process economics unless the goal is to obtain the maximum hydrogen possible from coal.

Note that the calculations above have been presented assuming an average current density across the cell. However, devices such as solid oxide electrolyzers and fuel cells are also chemical reactors in which the current density varies with gas compositions and thus non-isothermal devices. A detailed transport model that couples multiple transport phenomena would be required to obtain the details of these variations [24].

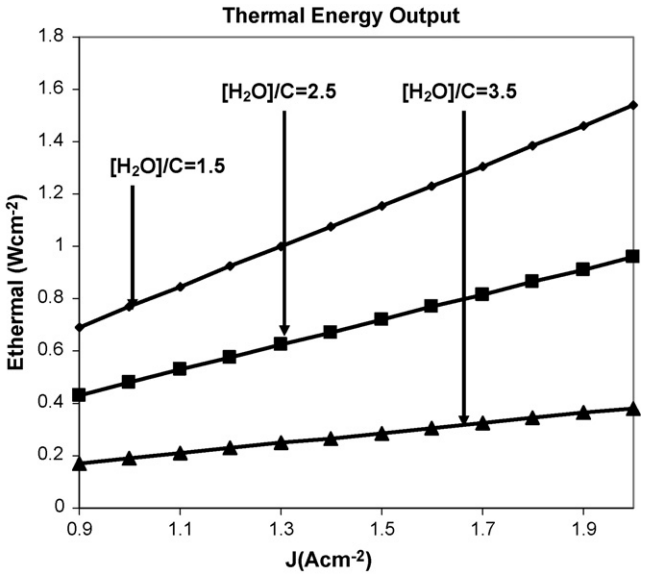

Fig. 5. Thermal energy as a function of current density for various steam-to-carbon ratios.

2.2. Analysis of the fuel cell efficiency

The fuel cell part of the proposed device will essentially function in the same way as the current state of the art tubular SOFCs. For a base line comparison, one can start by using the efficiency figures available for the Siemens Westinghouse state of the art tubular SOFCs [23]. It is reported that if a SOFC is pressurized, an increased voltage results, leading to improved performance. For example, operation at 3 atm could increase the power output by ∼10%. However, this improved performance alone may not justify the expense of pressurization, but what may is the ability to integrate the SOFC with a gas turbine (GT), which needs a hot pressurized gas flow to operate. Since the SOFC stack operates at 1000 °C (1273 K) it produces a high temperature exhaust gas. If operated at an elevated pressure, the exhaust becomes a hot pressurized gas flow that can be used to drive a turbine. If a SOFC is pressurized and integrated with a gas turbine, the pressurized air needed by the SOFC can be provided by the gas turbine's compressor, the SOFC can act as the system combustor, and the exhaust from the SOFC can drive the compressor and a separate generator. This yields a dry (no steam) hybrid-cycle power system that can have very high electrical generation efficiency. Analysis indicates that with such SOFC/GT hybrids an electrical efficiency of 55% can be achieved at power plant capacities as low as 250 kW, and ∼60% as low as 1 MW using small gas turbines. At the 2–3 MW capacity level with larger, more sophisticated gas turbines, analysis indicates that electrical efficiencies of up to 70% are possible [25].

The major difference between the proposed SOFC and the state of the art tubular SOFCs based on YSZ electrolyte is the choice of the cathode material; state of the art tubular SOFCs are either cathode or anode supported. The proposed SOFC will utilize liquid silver as the cathode whereas the state-of-the-art SOFCs employ Sr-doped lanthanum manganite (LSM) as the cathode. It is expected that liquid silver in the proposed SOFC will provide a larger interfacial area with the YSZ electrolyte for the charge-transfer reaction compared to the LSM/YSZ interfacial area in the state of the art tubular SOFCs. Furthermore, the electronic conductivity of silver is much larger compared to LSM and the oxygen diffusivity in molten silver is also relatively high. As a result, it is expected that polarization losses at the molten silver cathode in the proposed SOFC will be lower than the state of the art tubular SOFCs. In conclusion, it is believed that the proposed SOFC architecture (device) will have a better performance compared to the state of the art tubular SOFCs while also being reversible as an electrolyzer and therefore the efficiencies envisioned are expected to be higher.

In principle, the gasified feed from a coal gasifier can be fed directly to a SOFC. In principle, if the SOFC is operated at a high fuel utilization (greater than 90%) on gasified feed from a coal gasifier, it is possible to burn the remaining fuel in a small amount of oxygen and sequester the resulting CO_2 after condensing the H_2O from the depleted fuel stream. However, operating the fuel cell at very high fuel utilization leads to very high water vapor pressure on the anode side which in turn results in a high vapor pressure of volatile $Ni(OH)_2$, and loss of nickel from the anode. Further, the purpose of the proposed device is to eliminate the gasifier by incorporating dual-functionalities, i.e. as an electrolyzer and as a fuel cell.

3. Conclusions

A novel device for a reversible solid oxide fuel cell—electrolyzer based on a liquid metal electrode has been proposed and analyzed. The device based on coal as a fuel would employ a liquid metal electrode functioning as the anode in the electrolyzer mode and as the cathode in the fuel cell mode. In the electrolyzer mode hydrogen is generated from coal and in the fuel cell mode the hydrogen is consumed to generate electricity by the same device. The Ni–YSZ cermet electrode serves as the cathode in the electrolyzer mode and as the anode in the fuel cell mode. Calculations have been presented for different assumed values of the area specific ohmic and polarization resistances of the cell and for various steam-to-carbon ratios. It is shown that the hydrogen generation efficiency is a strong function of the total area specific resistance of the cell but is not a function of the steam-to-carbon ratio. By contrast, the overall efficiency of the system is a strong function of both the area specific resistance and the steam-to-carbon ratio. With increasing steam-to-carbon ratio, the net thermal energy output from the heat exchanger decreases and thus the overall energy efficiency of the process decreases.

References

[1] W.T. Thompson, Bull. Alloy Phase Diagr. 9 (3) (1988) 226.
[2] K.E. Oberg, L.M. Friedman, W.M. Boorstein, R.A. Rapp, The diffusivity and solubility of oxygen in liquid copper and liquid silver from electrochemical measurements, Metall. Trans. 4 (1973) 61.
[3] A.J. McEvoy, Oxygen diffusion through silver cathodes for solid oxide fuel cells, J. Phys. Chem. Solids 55 (1994) 339.

[4] A. Roine, HSC Thermodynamic Software, fifth ed., Outokumpo Research Oy, Pori, Finland, 2003.
[5] S. Primdahl, M. Mogensen, Oxidation of hydrogen on Ni/yttria-stabilized zirconia cermet anodes, J. Electrochem. Soc. 144 (1997) 3409.
[6] J. Mizusaki, H. Tagawa, T. Saito, T. Yamamura, K. Kamitani, K. Hirano, S. Ehara, T. Takagi, T. Hikita, M. Ippommatsu, S. Nakagawa, K. Hashimoto, Kinetic studies of the reaction at the nickel pattern electrode on YSZ in H_2–H_2O atmospheres, Solid State Ionics 70/71 (1994) 52.
[7] A. Krishnan, X.G. Lu, U.B. Pal, Solid oxide membrane (SOM) technology for cost-effective and environmentally sound production of metals and alloys from their oxide sources, in: EPD Congress, TMS Publication, 2005, p. 455.
[8] A. Krishnan, X.G. Lu, U.B. Pal, Solid oxide membrane (SOM) for cost effective and environmentally sound production of magnesium directly from magnesium oxide, in: Magnesium Technology, TMS Publication, 2005, p. 7.
[9] U.B. Pal, A. Krishnan, T. Keenan, C.P. Manning, Solid-oxide-oxygen-ion-conducting membrane (SOM) technology for green synthesis of metals from its oxides, in: Proceedings of the High Temperature Materials Symposium in Honor of the 65th Birthday of Professor Wayne L. Worrell, ECS Publication, 2002, p. 94.
[10] U.B. Pal, A. Krishnan, C.P. Manning, Zirconia-based inert anodes for green electro-synthesis of metals and alloys, in: Proceedings of the Yazawa International Symposium on Metallurgical and Materials Processing, TMS Publication, 2003, p. 351.
[11] A. Krishnan, X.G. Lu, U.B. Pal, Solid oxide membrane process for magnesium production directly from magnesium oxide, Metall. Mater. Trans. 36B (2005) 463.
[12] Wenquan Gong, Srikanth Gopalan, U.B. Pal, Polarization study on doped lanthanum gallate electrolyte using impedance spectroscopy, J. Mater. Eng. Perform. 13 (June (3)) (2004) 274.
[13] W. Gong, S. Gopalan, U.B. Pal, Cathodic polarization study on doped lanthanum gallate electrolyte using impedance spectroscopy, J. Electroceram. 13 (2004) 653.
[14] S.P. Jiang, J.G. Love, J.P. Zhang, M. Hoang, Y. Ramprakash, A.E. Hughes, S.P.S. Badwal, The electrochemcial performance of LSM/zirconia-yttria interface as a function of A-site non-stoichiometry and cathodic current treatment, Solid State Ionics 121 (1999) 1.
[15] S. Wang, X. Lu, M. Liu, Electrocatalytic properties of LSM-based electrodes for oxygen reduction, J. Solid State Electrochem. 6 (2002) 384.
[16] A. Petric, P. Huang, F. Tietz, Evaluation of La–Sr–Co–Fe–O perovskites for solid oxide fuel cells and gas separation membranes, Solid State Ionics 35 (2000) 719.
[17] FutureGen Website, http://www.netl.doe.gov/coal/futuregen/index.html.
[18] Solid State Energy Conversion Alliance Website, www.http://seca.doe.gov.
[19] T.A. Ramanarayanan, R.A. Rapp, The diffusivity and solubility of oxygen in liquid tin and solid silver and the diffusivity of oxygen in solid nickel, Metall. Trans. 3 (1972) 3239.
[20] W. Gong, Materials system for intermediate temperature solid oxide fuel cells based on doped lanthanum–gallate electrolyte, Ph.D. Thesis, Boston University, Boston, MA, 2005.
[21] A. Krishnan, Solid oxide membrane cell for oxide (MgO) electrolysis and metal (Mg) production, PhD Thesis, 2005. Boston University, Boston, MA.
[22] J. Martinez-Frias, A.-Q. Pham, S.M. Aceves, A natural gas assisted steam electrolyzer for high efficiency production of hydrogen, Int. J. Hydrogen Energy 28 (5) (2003) 483.
[23] D. Ragone, Thermodynamics of Materials, vol. 1, Wiley, New York, 1995, p. 153.
[24] P.-W. Li, M.K. Chyu, J. Power Sources 124 (2003) 487–498.
[25] Siemens-Westinghouse http://www.siemenswestinghouse.com/en/fuelcells/hybrid/index.cfm.